ARTICLE IN PRESS

Scientific Data

https://doi.org/10.1038/s41597-026-06781-8

Article in Press

RadRepro CBCT: An Open-Access CBCT Phantom Dataset for Improved Standardization and Reproducibility of Radiomics Research

Received: 17 April 2025

Accepted: 31 January 2026

Cite this article as: Hatamikia, S., Steiner, E., Muniya, E.J. *et al.* RadRepro CBCT: An Open-Access CBCT Phantom Dataset for Improved Standardization and Reproducibility of Radiomics Research. *Sci Data* (2026). https://doi.org/10.1038/s41597-026-06781-8

Sepideh Hatamikia, Elisabeth Steiner, Eashrat Jahan Muniya, Soraya Elmirad, Arezoo Borji, Gernot Kronreif, Wolfgang Birkfellner & Martin Buschmann

We are providing an unedited version of this manuscript to give early access to its findings. Before final publication, the manuscript will undergo further editing. Please note there may be errors present which affect the content, and all legal disclaimers apply.

If this paper is publishing under a Transparent Peer Review model then Peer Review reports will publish with the final article.

ARTICLE IN PRESS

© The Author(s) 2026. **Open Access** This article is licensed under a Creative Commons Attribution-NonCommercial-NoDerivatives 4.0 International License, which permits any non-commercial use, sharing, distribution and reproduction in any medium or format, as long as you give appropriate credit to the original author(s) and the source, provide a link to the Creative Commons licence, and indicate if you modified the licensed material. You do not have permission under this licence to share adapted material derived from this article or parts of it. The images or other third party material in this article are included in the article's Creative Commons licence, unless indicated otherwise in a credit line to the material. If material is not included in the article's Creative Commons licence and your intended use is not permitted by statutory regulation or exceeds the permitted use, you will need to obtain permission directly from the copyright holder. To view a copy of this licence, visit http://creativecommons.org/licenses/by-nc-nd/4.0/.

ARTICLE IN PRESS

RadRepro CBCT: An Open-Access CBCT Phantom Dataset for Improved Standardization and Reproducibility of Radiomics Research

Sepideh Hatamikia[1, 2, 3]*, Elisabeth Steiner [4], Eashrat Jahan Muniya [3], Soraya Elmirad [4],

Arezoo Borji [3 2,1], Gernot Kronreif [3], Wolfgang Birkfellner [2], Martin Buschmann [5]

[1]Clinical AI-Research in Omics and Medical Data Science (CAROM) group, Department of Medicine, Danube Private University (DPU), Krems, Austria

[2]Center for Medical Physics and Biomedical Engineering, Medical University of Vienna, Vienna, Austria

[3]Austrain Center for Medical Innovation and Technology (ACMIT), Wiener Neustadt, Austria

[4]Clinical Institute for Radiation Oncology and Radiotherapy, University Hospital Wiener Neustadt, Wiener Neustadt, Austria

[5]Department of Radiation Oncology, Medical University of Vienna/University Hospital Vienna, Austria

* Corresponding author

Email corresponding author: sepideh.hatamikia@dp-uni.ac.at

ARTICLE IN PRESS

Abstract

Radiomics, the extraction of quantitative features from medical images, has shown great potential in improving precision diagnosis, prognosis, and treatment planning. However, the reproducibility of radiomics features remains a major challenge due to the variability introduced by differences in imaging devices, acquisition protocols, and image reconstruction methods. This study introduces the first open-access cone-beam computed tomography (CBCT) phantom dataset specifically designed to test reproducibility in on-board imaging systems used in C-arm linear accelerators for radiotherapy. Using a widely recognized Catphan phantom, CBCT images were acquired from multiple devices across different imaging parameters, including variations in mAs, slice thickness, and reconstruction filters. The dataset includes 120 CBCT volumes with corresponding region of interest (ROI) segmentations and radiomics features enabling comprehensive testing of radiomics feature stability across intra- and inter-vendor comparisons. By providing this open-access dataset, the study aims to facilitate the standardization of CBCT radiomics research, improve feature reproducibility, and support the development of robust radiomics models for clinical applications.

Keywords: CBCT, Radiomics, Reproducibility, Phantom, Open access data, Linear accelerator

ARTICLE IN PRESS

Background & Summary

Radiomics is an emerging field that leverages advanced computational techniques to extract quantitative features from medical images, facilitating the identification of imaging biomarkers for precision diagnosis, prognosis, and treatment planning [1-3]. By mining vast amounts of data from radiological images, radiomics offers a powerful method for analyzing tumor heterogeneity and other disease-related characteristics [4, 5, 6]. However, despite its potential, the generalizability and reproducibility of radiomics features are currently very limited due to the sensitivity of these features to variations in image acquisition parameters and differences between imaging systems [7-11]. Therefore, radiomics features, such as those derived from texture analysis, intensity histograms, and morphological measurements, can be influenced by factors like scanner type, slice thickness, image resolution, and reconstruction algorithms [7-11]. These inconsistencies lead to substantial variability between studies, limiting the clinical application of radiomics. For example, differences in slice thickness or reconstruction algorithms can dramatically affect radiomic measurements, even for the same patient scanned under slightly different conditions. These issues are further exacerbated by the fact that many radiomics studies lack standardization in imaging protocols, image normalization, and feature extraction methods. This lack of standardization can lead to bias, false findings, and challenges in comparing results across studies.

CBCT is increasingly used in various clinical domains due to its real-time 3D imaging capability, compact hardware, and integration with treatment or surgical systems. In image-guided surgeries, particularly in orthopedics, dental and maxillofacial procedures, and neurosurgery, CBCT enables precise localization and verification of anatomical targets during interventions. Its intraoperative use enhances surgical accuracy and reduces the need for repeat procedures. In interventional radiology, CBCT is used for guidance during procedures such as tumor ablation, embolization, and biopsy, allowing clinicians to visualize vascular structures and soft tissue targets with minimal invasiveness. In oncology, CBCT plays a central role in image-guided radiotherapy (IGRT), where it is used for daily patient setup verification, treatment adaptation, and monitoring anatomical changes such as tumor shrinkage, weight loss, or organ motion throughout the treatment course. In adaptive radiotherapy, CBCT data is used to inform re-planning when anatomical changes affect dose distribution, thereby improving treatment precision and sparing healthy tissue.

Beyond its foundational role in radiotherapy, CBCT has recently gained interest as a source for radiomics analysis [12-24]. CBCT imaging is widely available and provides the opportunity to collect serial imaging data during the course of treatment. This makes it a valuable tool for monitoring treatment-induced changes in patients, particularly in cancer therapy. CBCT's repeated imaging capability during treatment

ARTICLE IN PRESS

enables the extraction of temporal radiomics features, which can be correlated with biological changes and treatment response. Several studies have demonstrated the utility of CBCT-based radiomics for predicting therapy response and clinical outcomes in different cancer types. For example, several studies have highlighted the potential of CBCT radiomics for predicting treatment outcomes, such as the prediction of xerostomia in head and neck cancer patients [19, 20], prediction or radiotherapy response in different types of cancers [17, 21-23] and survival prediction of cancer using radiomics analyses of CBCT images [18, 25]. Apart from the sensitivity of radiomics features to different scanner types, imaging parameters, feature extraction software, and normalization methods factors which limit radiomics reproducibility as with other imaging modalities [12-16] the use of CBCT images in radiomics research presents a unique challenge. Due to the design of CBCT systems, which utilize flat-panel detectors, these images are prone to higher scatter and lower quality compared to diagnostic CT scans, making radiomic feature stability a significant concern.

Given the existing limitations and challenges, a critical need exists for datasets that can facilitate the reproducibility and standardization of radiomics features derived from CBCT images. Open-access datasets, particularly those utilizing phantom images, offer an invaluable resource for testing, comparing, and harmonizing radiomic features across different imaging systems and acquisition protocols. Phantoms, unlike patient data, provide a controlled environment where imaging parameters can be systematically varied, allowing researchers to isolate and measure the impact of specific factors on radiomic feature stability. To the best of our knowledge, no publicly available CBCT dataset specifically designed for radiomics reproducibility research currently exists. The only study that proposed a dataset for this purpose used different phantoms and imaging data acquired at three centers, collected specifically to investigate reproducibility in radiomics [26]. While that dataset is very valuable for testing the stability of radiomic features under varying acquisition settings, scanners, and reconstruction algorithms, it was based on CT imaging rather than CBCT. In addition, another CT dataset has been introduced using a 3D-printed phantom derived from real patient data, which enabled systematic evaluation of reconstruction algorithm parameters, kernels, slice thickness, and slice spacing [27]. Given the inherent differences in image quality and noise characteristics between CT and CBCT and the strong influence these factors have on radiomic features a dedicated CBCT radiomics dataset is of significant value.

To address this gap, we present the first open-access CBCT phantom dataset aimed at advancing radiomics reproducibility research. This dataset allows researchers to test the robustness of radiomic features under different imaging conditions within the used scanners itself and also to compare this reproducibility results with data from other imaging systems they may have access to, enabling the identification of stable and reproducible features that can be used reliably in the clinical setting. By providing this resource, we aim to contribute to the growing body of work focused on improving the standardization and reproducibility of radiomics-based research, with the ultimate goal of enhancing its clinical utility.

Methods

Catphan Phantom

ARTICLE IN PRESS

The Catphan 503 phantom (Phantom Laboratory, Salem, NY) was used for all scans. The Catphan phantom is a test object designed for the measurement of image quality metrics on CT and CBCT scanners. It features test modules for sensitometry, uniformity, geometric and low contrast sensitivity performance [28]. The phantom has a cylindrical shape (diameter 20 cm), however, an oval-shaped body annulus (25-35 cm diameter) was put on the cylinder to simulate a typical human body shape.

One of the key advantages of the Catphan phantom in the context of radiomics reproducibility is its widespread availability in clinical settings, particularly those using C-arm linear accelerators. The two major linac vendors Elekta (Elekta AB, Stockholm Sweden) and Varian (Varian Medical Systems, Palo Alto, CA) typically supply Catphan phantoms alongside their CBCT systems, making it a common and accessible tool across many institutions. This broad distribution facilitates reproducibility and benchmarking, as clinics can directly compare their radiomics measurements with those reported in studies using the same phantom. Such consistency in phantom use enhances the generalizability and clinical relevance of radiomics research outcomes. Therefore, we selected this phantom because of it such widely use, allowing data acquisition across different vendors and enabling direct comparisons when other researchers use the same phantom. This facilitates benchmarking and enhances the reproducibility of results.
Additionally, the Catphan phantom was utilized in a previous study for CBCT radiomics analysis with a similar segmentation approach (see image annotation section) [29]. Its standardized structure makes it a valuable tool for assessing imaging performance and the reproducibility of radiomics features. The 503 version of the Catphan phantom is distributed by Elekta, whereas a variation of the Catphan phantom is distributed by Varian. These represent the two major C-arm linac vendors. The Catphan 503 phantom, was selected for this study to ensure consistency across all imaging platforms. While the Catphan 504 and 604 are more commonly used with Varian CBCT systems, our experiments were initially designed and conducted using Elekta devices. To maintain standardization and comparability across vendors, we chose to use the same phantom, Catphan 503, for all scans, including those performed on Varian systems. This approach was critical given the study's focus on radiomics feature reproducibility, where even small differences in phantom design could impact the results.

ARTICLE IN PRESS

Image Acquisition Protocols

CBCT acquisitions of the Catphan phantom were performed on different CBCT scanners:

1) The Elekta X-ray volume imager (XVI, Version 5.0) was used in this study which is an on-board CBCT imaging system on Elekta radiotherapy linacs. It features a flat-panel image detector and the detector-source distance was 153.6cm. The image receptor size was 41×41cm2 and provided an image size of 1024×1024 pixels, however, clinical protocols usually used 512 pixels. The system used a 16-bit pixel grayscale resolution. The total filtration for the X-ray tube was 7.0 mm Al equivalence at 100 kV. A bow-tie filter was used for all scans on Elekta systems in this study. The CBCT reconstruction in Elekta XVI employed the Feldkamp-Davis-Kress (FDK) back projection algorithm together with a Wiener filter. Pre-processing filters could be applied on the projections. Three similar Elekta CBCT devices were used in this study. Two systems featured the software version 5.04 and one system version 5.07.

2- Varian radiotherapy system (TrueBeam Version 4.1) was also used in this study which is an on-board kV imager for CBCT imaging. The system includes a flat-panel image detector (PaxScan4030CB) of 30 x 40 cm^2 with a source-to-imager distance of 100 cm at isocenter and a source-to-axis distance of 100 cm. The field

ARTICLE IN PRESS

size ranges from 2 × 2 cm to 50 × 50 cm, with a default image matrix size of 512 × 512 pixels. The X-ray tube has an inherent filtration of 2.7 mm Al at 75 kV. Additionally, the kV beam delivery system utilizes two types of filters: a beam-hardening foil filter (0.89 mm thick titanium) to optimize the X-ray energy spectrum and bowtie filters (Full-Fan for head scans, Half-Fan for body scans) to enhance CBCT projection quality. Varian system also used FDK algorithm for CBCT reconstruction.

Figures 1 and 2 represent the CBCT scanners used in this study and the setup with Catphan phantom for image acquisition.

The selection of these three scanners was conducted by the following objectives:

1. **Intra-vendor comparison:** The inclusion of three Elekta XVI scanners allowed for the acquisition of identical measurements, enabling a direct comparison of radiomics features across different imaging devices from the same vendor.
2. **Inter-vendor comparison:** When performing measurements on scanners from different vendors, such as Elekta and Varian, achieving identical imaging parameters was not feasible due to each vendor's unique predefined protocols and imaging settings. However, every effort was made to match acquisition and imaging parameters as closely as possible. The aim was to provide an open-access dataset that allows researchers to assess the reproducibility of radiomics features across different vendors when imaging parameters vary. For instance, one can assess the stability of radiomics features by varying the exposure (mAs) on the Elekta system (within a possible range for predefined protocols of the imaging vendor) and comparing the reproducibility level of these features—rather than their absolute values—with those obtained from the Varian system. This analysis provides valuable insights into how different image acquisition settings at different CBCT imaging vendors impact radiomics feature consistency.

Various imaging setup were conducted, including varying slice thickness, exposure (mAs values), and the use of different pre-filters before reconstruction. Additionally, a test-retest protocol was implemented on each scanner to evaluate intrascanner repeatability. Furthermore, the phantom was deliberately shifted in different directions to assess the impact of positioning on the extraction of radiomics features in CBCT imaging. Shifts in different directions were introduced during image acquisition to mimic changes in the target object's location within the field of view. This was motivated by prior evidence that object location may influence both grey-value accuracy and the reproducibility of radiomic features in CBCT [30, 31, 32]. By applying these shifts, we aimed to investigate potential location-related variability in radiomic feature stability.

Figure 1. Measurement setups for Elekta XVI system at Department of Radiation Oncology, Medical University of Vienna/University Hospital Vienna, Austria.

ARTICLE IN PRESS

Figure 2. Measurement setups for Varian TrueBeam system with Cathphan phantom at University Hospital Wiener Neustadt, Austria.

The Chest/Thorax protocol was chosen because the default scan parameters for this region were highly similar across the two vendor CBCT systems used in this study. In addition, many of the most influential radiomics studies have been performed on lung CTs, and several large, publicly available lung radiomics datasets exist [33–35]. The thorax represents a promising site for CBCT/CT radiomics research owing to the pronounced contrast between lung and tumor tissues, which supports reliable segmentation and feature extraction. Future studies will include exploring and optimizing scanning protocols for other anatomical regions and tumor sites.

The complete details on acquisition protocol used is described as follow and in Table 1:

Elekta Device 1

- Exposure (mAs) variable: the acquisitions were performed at 120 kV, changing the mAs parameter with following values 127, 169, 211, 264, 330, 412, 528 mAs.
- Slice thickness variable: the reconstructions were performed at four different slice thickness including 1mm, 2mm, 3mm and 4mm.
- Pre-filters before reconstruction variable: two filters were applied to projection images before reconstruction including None, Despeckle and Median 5. The Despeckle filter removed speckles from the projection images before 3D reconstruction. The median5 filter applied a median window of a pixel and the four adjacent pixels on the projections.
- Test-retest: the measurements were repeated 10 times on an initial scan

ARTICLE IN PRESS

- Shift: the measurements were repeated 6 times on an initial scan, by applying 3 centimeter shift each in three directions (vertical (up, down), longitudinal (front, back) and lateral (right, left))
- The Protocol used was “Chest M20”, which is the vendor default Chest CBCT protocol and used 120 kV beam energy.

Varian Device 2

- Exposure (mAs) variable: the acquisitions were performed at 125 KV, changing the mA parameter with following values: 123, 168, 224, 269, 337, 403, 537 mAs.
- Slice thickness variable: reconstruction were performed at four different slice thickness including 1mm, 2mm, 3mm and 4mm.
- Pre-filters before reconstruction: three filters were applied to projection images before reconstruction including Smooth, Sharp, Ultra Sharp
- Test-retest: the measurements were repeated 10 times on an initial scan
- Shift: the measurements were repeated 6 times on an initial scan, by applying 3 centimeter shift each in three directions (vertical (anterior, posterior), longitudinal (carinal, caudal) and lateral (right, left))
- The protocol used was “Thorax” which is the vendor default standard reconstruction Thorax CBCT protocol and used 120 kV beam energy.

For each device, imaging sequences were acquired using seven different mAs settings, four slice thicknesses, three pre-filters, ten test-retest scans, and six positional shifts, resulting in a total of 30 3D volumes per scanner (Table 1). Consequently, across the four scanners, a total of 120 volumes were collected. The complete protocol for each device was conducted in a single session. The overall study design is illustrated in Figure 3. The default clinical Chest/Thorax scanning protocol (approximately 270 mAs exposure) was used as the baseline for image acquisition. To assess radiomics feature reproducibility under slightly different imaging conditions, modest variations in exposure were applied in both directions (increased and decreased mAs). The default protocols were chosen because they are representative of common clinical practice across institutions, providing a relevant reference for evaluating radiomics robustness. All registered scans within each device group (Elekta and Varian) had identical native voxel spacing including consistent in-plane resolution (1.0 × 1.0 mm for Elekta and 0.908 × 0.908 mm for Varian), no resampling was required.

Parameters / *Device*	*Exposure(mAs)*	*Slice Thickness*	*Pre-filters*
Elekta	*120 KV -> 127, 169, 211, 264, 330, 412, 528 mAs*	*1mm,2mm, 3mm, 4mm*	*None, Despeckle, Median 5*
Varian	*125KV -> 123, 168, 224, 269, 337, 403, 537 mAs*	*1mm,2mm, 3mm, 4mm*	*Smooth, Sharp, Ultra Sharp*

Table 1: Device-specific CBCT acquisition parameters and imaging variation ranges.

Image Registration

For each device, all scans were 3D registered to an initial reference scan to ensure consistency across the dataset. Image registration was performed using the open-source medical image analysis platform 3D Slicer (version 4.10, http://www.slicer.org). The scanned images were imported in Digital Imaging and Communication in Medicine (DICOM) format. The general registration (BRAINS) module in 3D Slicer was used for the registration process, applying rigid, affine, scaling, and skew transformations with 12 degrees of freedom (DOF). The "useGeometryAlign" option was utilized to initialize the transform node. All the registered scans have same voxel spacing matching the fixed scan ensuring consistency across the dataset for each device.

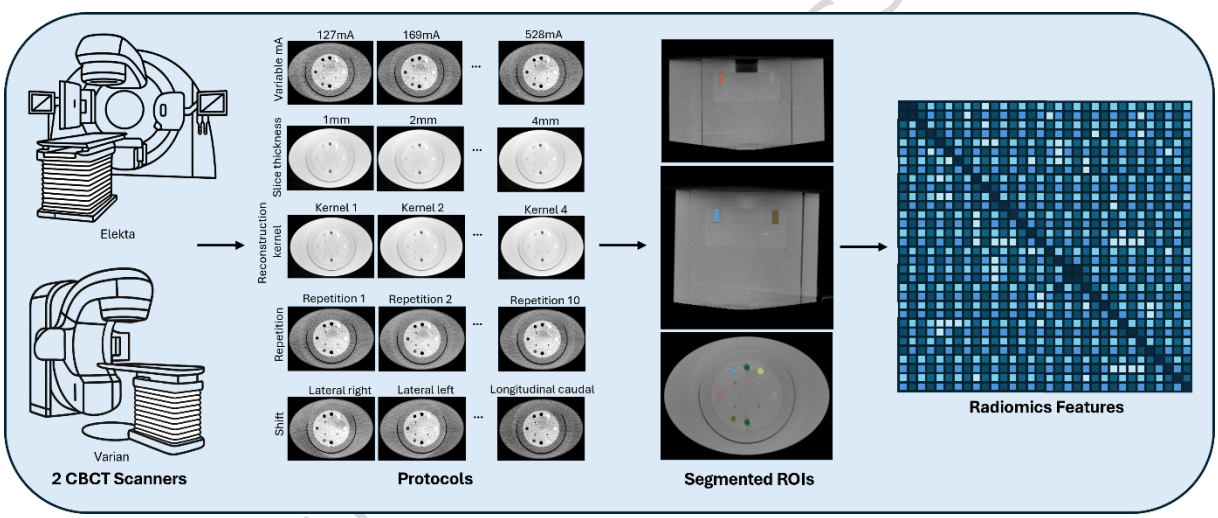

Figure 3. Study design. The images were acquired on CBCT scanners from two imaging vendors i.e., Elekta and Varian. Different variation in mA, slice thickness, reconstruction kernel, repetition and shift were used. The Segmented ROIs are obtained manually similar to [29].

Image Annotation

For each device, regions of interest (ROIs) were created to serve as the basis for radiomic feature extraction. Six ROIs were defined as binary masks, representing materials with known densities, consistent with the materials described in [29]. Cylindrical 3D objects were generated in 3D Slicer to segment the ROIs corresponding to Delrin, Polystyrene, Low-Density Polyethylene (LDPE), Polymethylpentene (PMP), and Air, each using a cylinder of 22 × 10 mm, while Teflon was segmented using a 22 × 12 mm cylinder. These dimensions were selected to ensure that the cylinder boundaries remained fully contained within each material compartment.

The cylindrical ROIs were initially created automatically, and manual transformation was applied using the Transforms module in 3D Slicer to precisely align each cylinder with the anatomical location of its

ARTICLE IN PRESS

corresponding material. Following this alignment, all scans were rigidly registered to a single reference scan (see Image Registration section). This allowed the same cylindrical ROIs, in fixed spatial coordinates, to be applied consistently across all registered scans without the need for repeated segmentation. As a result, the process avoided intra- or inter-observer variability and ensured full reproducibility of the ROIs used for radiomic feature extraction.

The final annotated segmentations are shown in Figure 4, and the corresponding ROI binary masks are provided together with the image data (see Data Record section).

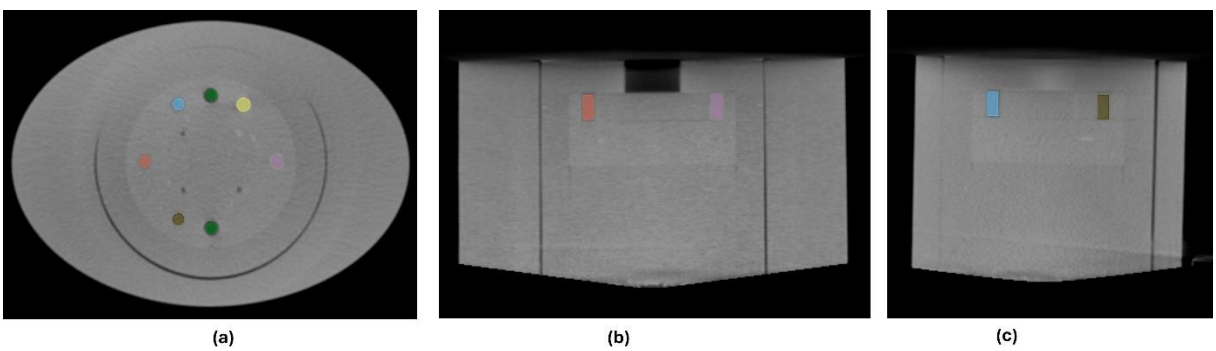

Figure 4. Axial (a), Sagittal (b) and Coronal (c) slice of an example CBCT scan from Varian TrueBeam system. Segmented ROIs are shown in different colours for materials Teflon (yellow), Delrin (purple), Polystyrene (brown), LDPE (orange), PMP (blue) and Air (green).

ARTICLE IN PRESS

Radiomics Feature Extraction

We used MIRP (a python package for quantitative analysis of medical images) for extraction of radiomics features [36]. All CBCT images are discretized using a fixed bin size technique that was implemented in the MIRP library to guarantee IBSI-compliant radiomics feature extraction. Between −1000 and 3000 HU was the maximum intensity range, and a bin width of 25 HU was used. To prevent dataset-specific variability in bin placement, this fixed global range made sure that the lower edge of the first bin was always anchored at −1000 HU across all scans and regions of interest. All radiomics features were extracted in 3 dimension (3D). Since the through-plane resolution varied based on slice thickness (1–4 mm) and the in-plane voxel resolution was consistent across vendors (1.0 × 1.0 mm for Elekta, 0.908 × 0.908 mm for Varian), we resampled all CBCT volumes to isotropic 1 × 1 × 1 mm voxel spacing before feature extraction. The CBCT images were resampled using B-spline interpolation, and the binary ROI masks were resampled using nearest-neighbor interpolation to prevent partial volume effects. Consistent 3D texture analysis was made possible by this, which guaranteed that the rectilinear distances between adjacent voxels were uniform in all directions. To ensure reproducibility and compliance with IBSI guidelines, our published feature extraction scripts apply isotropic resampling prior to computation, even though the publicly available dataset is distributed in its original native resolution to preserve scanner fidelity. After being extracted, 107 radiomics features were divided into three primary categories: texture features, shape-based features, and first-order statistics. Gray Level Co-occurrence Matrix (GLCM), Gray Level Run Length Matrix (GLRLM), Gray Level Size Zone Matrix (GLSZM), and Gray Level Dependence Matrix (GLDM) were among the matrix

ARTICLE IN PRESS

types used to further group the texture features. Table 1 in Supplementary file summarizes the entire list of extracted features, arranged by feature type, feature category, and their estimated feature names.

Data Records

The complete dataset of 120 CBCT images obtained with 4 different CBCT scanners (two vendors), for different tube current, pre-filtering before reconstruction, slice thickness as well as test-retest and shift which are all available at the following Zenodo repository [37]. 3D Slicer was used to convert the DICOM files to NIfTI format to guarantee ease of use of our phantom scans with different software tools. The repository consists of folders named “Elekta_LinacB/D/E” and “Varian” include all the CBCT images saved as NIfTI format. All files are named in the following format: “CBCTscanner_TubeCurrent_Slice-Thickness/Pre-Filter-Reconstruction/Test-Retest/Shift/Protocol.nii.gz”. The folder “ROI” inside each device contains the complete set of cylinder segmentations as binary label maps of the ROIs inside the scans of the Catphan phantom, which are also saved in NIfTI format and labeled as “Devicenumber_ROI_name.nii.gz”. The Folder “Radiomics” contains the corresponding radiomics features of each scan. The files are named in the following format: “CBCTscanner_TubeCurrent_Slice-Thickness/Pre-Filter-Reconstruction/Test-Retest/Shift/Protocol_radiomics_features.cvs”.

Technical Validation

All four CBCT scanners used undergo regular maintenance and calibration, ensuring optimal performance. At both institutions, including the University Hospital Vienna, Department of Radiation Oncology and Radiotherapy, University Hospital Wiener Neustadt, Clinical Institute for Radiation Oncology and Radiotherapy where data collection took place, quality assurance is routinely conducted as part of standard patient care. The CBCT acquisition protocols were supported by experienced medical physicists who routinely work with these scanners in clinical settings.

It is important to note that while the selected ROIs do not precisely align with anatomical structures, they were strategically positioned within the image space to capture a diverse range of textures. This approach ensures that the extracted features from our phantom ROIs encompass a wide spectrum of feature values typically observed in clinical datasets. Therefore, we can reasonably infer that the analytical outcomes obtained from our phantom study are applicable in a clinical setting.

Usage Notes

The dataset will be available in the Zenodo repository [37] along with a brief description of its usage. All CBCT images and corresponding segmentations are provided in NIfTI format and can be visually inspected using various open-source medical image viewers, such as 3D Slicer, Analyze 7.5, and ITK-SNAP. To ensure reproducibility, radiomics feature extraction should be conducted using software that complies with IBSI standards [38]. The dataset is designed to support a wide range of radiomics reproducibility and benchmarking studies, as it includes controlled variations in mAs, slice thickness, reconstruction filters,

ARTICLE IN PRESS

scanner vendor, test–retest conditions, and phantom positioning. To facilitate immediate usability, we provide baseline radiomics results for all scans, including all extracted features, ROI masks, and the exact configuration files used for feature extraction. These resources enable researchers to benchmark their pipelines, evaluate feature stability, test harmonization or normalization strategies, and replicate our experiments without additional preprocessing. Example use cases which could benefit from our data include studying intra- and inter-vendor radiomics reproducibility, validating new radiomics pipelines, assessing the impact of acquisition variability, and more. All corresponding code is included in the Zenodo repository to ensure full reproducibility and to support transparent, standardized reuse of the dataset. In this study, we used Catphan phantom for all data acquisition. While the Catphan phantom offers the advantage of widespread availability and facilitates cross-institutional benchmarking, it does not replicate the anatomical complexity of human tissues. Therefore, future work should extend this dataset using anthropomorphic or 3D-printed patient-like phantoms to evaluate radiomics feature robustness under more clinically realistic conditions.

ARTICLE IN PRESS

Data availability

The data are published on Zenodo [37] (https://zenodo.org/records/18401318).

Code Availability

Code for Radiomics feature extraction is included in the Zenodo repository of the dataset in the file called CBCTRadiomicsCode.ipynb [37].

Acknowledgment

This study was funded by ACMIT COMET Module FFG project (FFG number: 879733, application number: 39955962) and Danube Private university (DPU).

Author contribution

S.H, M.B, E. S, G.K and W.B conceptualized the study, M.B, S.E and E.S performed the measurements and evaluation of them, S.H, E. JM and A.B did the analysis of the whole data and all authors contribute in writing and revising the paper.

Competing interests

The authors declare no competing interests.

References

[1] Lambin P, Rios-Velazquez E, Leijenaar R, Carvalho S, van Stiphout RG, Granton P, Zegers CM, Gillies R, Boellard R, Dekker A, Aerts HJ. Radiomics: extracting more information from medical images using advanced feature analysis. Eur J Cancer. 2012 Mar;48(4):441-6. doi: 10.1016/j.ejca.2011.11.036.

ARTICLE IN PRESS

[2] Parmar C, Grossmann P, Bussink J, Lambin P, Aerts HJWL. Machine Learning methods for Quantitative Radiomic Biomarkers. Sci Rep. 2015 Aug 17;5:13087. doi: 10.1038/srep13087.

[3] Afshar P, Mohammadi A, Plataniotis K. N, Oikonomou A, Benali H. From handcrafted to deep-learning-based cancer radiomics: challenges and opportunities, IEEE Signal Process. Mag. 2019 36: 132–160.

[4] Stanzione A, Ponsiglione A, Alessandrino F, Brembilla G, Imbriaco M. Beyond diagnosis: is there a role for radiomics in prostate cancer management? Eur Radiol Exp. 2023 Mar 13;7(1):13. doi: 10.1186/s41747-023-00321-4.

[5] Ibrahim A, Primakov S, Beuque M, Woodruff HC, Halilaj I, Wu G, Refaee T, Granzier R, Widaatalla Y, Hustinx R, Mottaghy FM, Lambin P. Radiomics for precision medicine: Current challenges, future prospects, and the proposal of a new framework. Methods. 2021 Apr;188:20-29. doi: 10.1016/j.ymeth.

[6] Schwarzhans F, George G, Escudero Sanchez L, Zaric O, Abraham JE, Woitek R, Hatamikia S. Image normalization techniques and their effect on the robustness and predictive power of breast MRI radiomics. Eur J Radiol. 2025 Jun;187:112086.

[7] Hatamikia S, George G, Schwarzhans F, Mahbod A, Woitek R. Breast MRI radiomics and machine learning-based predictions of response to neoadjuvant chemotherapy - How are they affected by variations in tumor delineation? Comput Struct Biotechnol J. 2023 Nov 19;23:52-63.

[8] Lee J, Steinmann A, Ding Y, Lee H, Owens C, Wang J, Yang J, Followill D, Ger R, MacKin D, Court LE. Radiomics feature robustness as measured using an MRI phantom. Sci Rep. 2021 Feb 17;11(1):3973. doi: 10.1038/s41598-021-83593-3.

[9] Hagiwara A, Fujita S, Ohno Y, Aoki S. Variability and Standardization of Quantitative Imaging: Monoparametric to Multiparametric Quantification, Radiomics, and Artificial Intelligence. Invest Radiol. 2020 Sep;55(9):601-616. doi: 10.1097/RLI.0000000000000666.

[10] Alberich-Bayarri A, Bellvís-Bataller (Eds.) F. Basics of Image Processing: the Facts and Challenges of Data Harmonization to Improve Radiomics Reproducibility, Springer International Publishing, Cham, 2023, https://doi.org/10.1007/978-3-031-48446-9.

[11] Traverso A, Wee L, Dekker A, Gillies R. Repeatability and Reproducibility of Radiomic Features: A Systematic Review. Int J Radiat Oncol Biol Phys. 2018 Nov 15;102(4):1143-1158. doi: 10.1016/j.ijrobp.2018.05.053.

[12] Wang H, Zhou Y, Wang X, Zhang Y, Ma C, Liu B, Kong Q, Yue N, Xu Z, Nie K. Reproducibility and Repeatability of CBCT-Derived Radiomics Features. Front Oncol. 2021 Nov 17;11:773512. doi: 10.3389/fonc.2021.773512.

[13] Xian He, Zhi Chen, Yutao Gao, Wanjing Wang, Meng You, Reproducibility and location-stability of radiomic features derived from cone-beam computed tomography: a phantom study, *Dentomaxillofacial Radiology*, Volume 52, Issue 8, 1 November 2023, 20230180,

ARTICLE IN PRESS

[14] Spuhler KD, Teruel JR, Galavis PE. Assessing the reproducibility of CBCT-derived radiomics features using a novel three-dimensional printed phantom. Med Phys. 2021 Aug;48(8):4326-4333.

[15] Delgadillo R, Spieler BO, Ford JC, Kwon D, Yang F, Studenski M, Padgett KR, Abramowitz MC, Dal Pra A, Stoyanova R, Pollack A, Dogan N. Repeatability of CBCT radiomic features and their correlation with CT radiomic features for prostate cancer. Med Phys. 2021 May;48(5):2386-2399. doi: 10.1002/mp.14787.

[16] Kathryn H. Brown, Neree Payan, Sarah Osman, Mihaela Ghita, Gerard M. Walls, Ileana Silvestre Patallo, Giuseppe Schettino, Kevin M. Prise, Conor K. McGarry, Karl T. Butterworth, Development and optimisation of a preclinical cone beam computed tomography-based radiomics workflow for radiation oncology research, Physics and Imaging in Radiation Oncology, Volume 26, 2023, 100446, ISSN 2405-6316,

[17] Delgadillo R, Deana AM, Ford JC, Studenski MT, Padgett KR, Abramowitz MC, Pra AD, Spieler BO, Dogan N. Increasing the efficiency of cone-beam CT based delta-radiomics using automated contours to predict radiotherapy-related toxicities in prostate cancer. Sci Rep. 2024 Apr 26;14(1):9563.

[18] van Timmeren JE, Leijenaar RTH, van Elmpt W, Reymen B, Oberije C, Monshouwer R, Bussink J, Brink C, Hansen O, Lambin P. Survival prediction of non-small cell lung cancer patients using radiomics analyses of cone-beam CT images. Radiother Oncol. 2017 Jun;123(3):363-369. doi: 10.1016/j.radonc.2017.04.016.

[19] Ismail M, Hanifa MAM, Mahidin EIM, Manan HA, Yahya N. Cone beam computed tomography (CBCT) and megavoltage computed tomography (MVCT)-based radiomics in head and neck cancers: a systematic review and radiomics quality score assessment. Quant Imaging Med Surg. 2024 Sep 1;14(9):6963-6977. doi: 10.21037/qims-24-334.

[20] Rosen BS, Hawkins PG, Polan DF, Balter JM, Brock KK, Kamp JD, Lockhart CM, Eisbruch A, Mierzwa ML, Ten Haken RK, El Naqa I. Early Changes in Serial CBCT-Measured Parotid Gland Biomarkers Predict Chronic Xerostomia After Head and Neck Radiation Therapy. Int J Radiat Oncol Biol Phys. 2018 Nov 15;102(4):1319-1329. doi: 10.1016/j.ijrobp.2018.06.048.

[21] Li Z, Raldow AC, Weidhaas JB, Zhou Q, Qi XS. Prediction of Radiation Treatment Response for Locally Advanced Rectal Cancer via a Longitudinal Trend Analysis Framework on Cone-Beam CT. Cancers (Basel). 2023 Oct 25;15(21):5142.

[22] Sellami S, Bourbonne V, Hatt M, Tixier F, Bouzid D, Lucia F, Pradier O, Goasduff G, Visvikis D, Schick U. Predicting response to radiotherapy of head and neck squamous cell carcinoma using radiomics from cone-beam CT images. Acta Oncol. 2022 Jan;61(1):73-80.

[23] Qin Q, Shi A, Zhang R, Wen Q, Niu T, Chen J, Qiu Q, Wan Y, Sun X, Xing L. Cone-beam CT radiomics features might improve the prediction of lung toxicity after SBRT in stage I NSCLC patients. Thorac Cancer. 2020 Apr;11(4):964-972.

[24] Hatamikia S, Oberoi G, Zacher A, Kronreif G, Birkfellner W, Kettenbach J, Ponti S, Lorenz A, Buschmann M, Jaksa L, Irnstorfer N, Unger E. Additively manufactured test phantoms for mimicking soft tissue radiation attenuation in CBCT using Polyjet technology. Z Med Phys. 2023 May;33(2):168-181.

ARTICLE IN PRESS

[25] Shi L, Rong Y, Daly M, Dyer B, Benedict S, Qiu J, Yamamoto T. Cone-beam computed tomography-based delta-radiomics for early response assessment in radiotherapy for locally advanced lung cancer. Phys Med Biol. 2020 Jan 10;65(1):015009. doi: 10.1088/1361-6560/ab3247.

[26] Kalendralis P, Traverso A, Shi Z, Zhovannik I, Monshouwer R, Starmans MPA, Klein S, Pfaehler E, Boellaard R, Dekker A, Wee L. Multicenter CT phantoms public dataset for radiomics reproducibility tests. Med Phys. 2019 Mar;46(3):1512-1518.

[27] https://www.cancerimagingarchive.net/collection/ct-phantom4radiomics/

[28] https://www.phantomlab.com/catphan-500

[29] Palani D, Shanmugam S, Govindaraj K. Analysing the possibility of utilizing CBCT radiomics as an independent modality: a phantom study. Asian Pac J Cancer Prev. 2021 May 1;22(5):1383-1391.

[30] He X, Chen Z, Gao Y, Wang W, You M. Reproducibility and location-stability of radiomic features derived from cone-beam computed tomography: a phantom study. Dentomaxillofac Radiol. 2023 Nov;52(8):20230180.

[31] Oliveira ML, Tosoni GM, Lindsey DH, Mendoza K, Tetradis S, Mallya SM. Influence of anatomical location on CT numbers in cone beam computed tomography. Oral Surg Oral Med Oral Pathol Oral Radiol 2013; 115: 558-564. doi: 10.1016/j.oooo.2013.01.021.

[32] Parsa A, Ibrahim N, Hassan B, van der Stelt P, Wismeijer D. Influence of object location in cone beam computed tomography (Newtom 5G and 3d Accuitomo 170) on gray value measurements at an implant site. Oral Radiol 2014; 30: 153–59. doi: 10.1007/s11282-013-0157-x.

[33] Aerts, H. J. W. L. et al. Decoding tumour phenotype by noninvasive imaging using a quantitative radiomics approach. Nat. Commun. 5:4006 doi: 10.1038/ncomms5006 (2014).

[34] Coroller et al. Radiomic phenotype features predict pathological response in non-small cell lung cancer. Radiother Oncol. 2016 Jun;119(3):480-6. doi: 10.1016/j.radonc.2016.04.004.

[35] Aerts, H. J. W. L., Wee, L., Rios Velazquez, E., Leijenaar, R. T. H., Parmar, C., Grossmann, P., Carvalho, S., Bussink, J., Monshouwer, R., Haibe-Kains, B., Rietveld, D., Hoebers, F., Rietbergen, M. M., Leemans, C. R., Dekker, A., Quackenbush, J., Gillies, R. J., Lambin, P. (2014). Data From NSCLC-Radiomics (version 4) [Data set]. The Cancer Imaging Archive. https://doi.org/10.7937/K9/TCIA.2015.PF0M9REI.

[36] Zwanenburg, A. and Löck, S. (2024) 'MIRP: A Python package for standardised radiomics', Journal of open source software, 9(99), p. 6413

[37] Hatamikia, S. et al. RadRepro CBCT: An Open-Access CBCT Phantom Dataset for Improved Standardization and Reproducibility of Radiomics Research. Zenodo https://doi.org/10.5281/zenodo.18401318 (2025).

ARTICLE IN PRESS

[38] Zwanenburg A, Vallières M, Abdalah MA, et al. The Image Biomarker Standardization Initiative: Standardized Quantitative Radiomics for High-Throughput Image-based Phenotyping. Radiology. 2020 May;295(2):328-338. doi: 10.1148/radiol.2020191145.

ARTICLE IN PRESS